

## Measurement of fission excitation functions in $^{11}\text{B}$ , $^{16}\text{O}$ , $^{19}\text{F}+^{232}\text{Th}$ reactions in the extreme sub-barrier energy region

D. M. Nadkarni, A. Saxena, D. C. Biswas, R. K. Choudhury, and S. S. Kapoor  
Nuclear Physics Division, Bhabha Atomic Research Centre, Mumbai-4000085, India

N. Majumdar and P. Bhattacharya  
Saha Institute of Nuclear Physics, I/AF, Bidhannagar, Calcutta-7000064, India

(Received 25 September 1998)

Fission cross sections have been measured for the systems of  $^{11}\text{B}$ ,  $^{16}\text{O}$ ,  $^{19}\text{F}+^{232}\text{Th}$  in the sub-barrier to extreme-sub-barrier energy (ESBE) region. Two position sensitive avalanche detectors were employed to measure the fission events due to fusion-fission (FF) and transfer fission (TF) processes using the fission fragment folding angle technique. The cross sections for fusion-fission reactions could be well accounted by the coupled channel calculations over a large energy range except in the ESBE region. The transfer induced fission cross sections are observed to be large at extreme sub-barrier energies. The ratio of transfer fission cross section to that of total fission is observed to increase rapidly as the energy is decreased in the sub-barrier region for all the systems. Also in the ESBE region a number of low momentum transfer fission (LMTF) events having folding angle close to  $180^\circ$  are observed with a rather weak dependence on the bombarding energy. These events were investigated by several control experiments. Considering the uncertainties involved in the control experiments, it appears difficult to rule out if they originate completely from background neutron induced reactions or from any new process such as Coulomb fission as conjectured in some earlier studies. The results on different components of the fission cross sections have been discussed. [S0556-2813(99)50201-X]

PACS number(s): 25.70.Hi, 25.70.Jj, 25.70.Bc

It is now well established that in many heavy-ion induced reactions, the fusion cross sections are significantly enhanced in the sub-barrier energy region as compared to the theoretical calculations based on simple one-dimensional barrier penetration models [1]. These models explain the observed cross sections at energies well above the fusion barrier ( $V_B$ ), but predict cross sections which are much lower than the observed values at below barrier energies. Subsequently, the sub-barrier enhancements in the fusion cross sections have been explained by incorporating several effects such as static deformation [2], zero-point vibration [3] of target and projectile nuclei, and by coupled channel formalism [4]. The coupled channel formalism leads to essentially a distribution of fusion barriers and thereby a resultant enhancement in the cross sections at the sub-barrier energies. The enhanced fusion cross section is attributed to the higher penetrability through the lower barriers in comparison to that expected for simple uncoupled one-dimensional barrier. In the case of highly fissile systems fission is the most dominant mode of decay, and fusion cross sections can be measured from the observed fission cross sections. The fission fragment folding angle technique can be used to decipher the components of fission arising due to fusion, transfer, and other low momentum transfer reactions. These features were exploited in the recent measurements [5,6] of fission cross sections for the systems of  $^{12}\text{C}$ ,  $^{16}\text{O}$ ,  $^{19}\text{F}+^{232}\text{Th}$  to obtain the experimental fusion barrier distributions for these systems, and the results were compared with the coupled channel calculations which included deformation and inelastic excitation of the target and projectile nuclei in the fusion process. Measurement of excitation functions down to the extreme sub-barrier energy (ESBE) region is important from the point of studying the long range behavior of nuclear interactions, and very little

data exist on the fission cross sections at the extreme sub-barrier energies. In Ref. [6], while carrying out the folding angle distribution measurements at the lowest energies, a large admixture of noncompound fission events was observed in various target-projectile systems. In particular at very low energies an extra peak was observed with folding angle of about  $180^\circ$  indicating a very low momentum transfer fission (LMTF) component which was conjectured to be due to the fission of Coulomb excited states of the target. The latter type of events were also postulated in an earlier work [7] to explain the enhanced fission cross sections in light projectile induced fission of uranium isotopes at extreme sub-barrier energies. Fission events attributed to Coulomb excited target fission were also reported [8] in a reverse reaction of uranium ion beam (1.2 MeV/nucleon) on  $^{208}\text{Pb}$  target carried out with super-HILAC at Berkeley. In another measurement [9] of  $^{10}\text{B}$  induced fission of  $^{235}\text{U}$  also, enhancements in the measured cross sections were observed as compared to that estimated with the Wong-Esbensen model [2,3] in the ESBE region. In all these above measurements solid state nuclear track detectors (SSNTD) were used for detecting fission events. In a subsequent work, Gehring *et al.* [10] reported the measurements of proton induced fission cross section of  $^{235}\text{U}$  employing the kinematic coincidence technique with a pair of gas avalanche counters and found that the observed cross sections were in agreement with the earlier [7] SSNTD measurements up to 3 MeV bombarding energy and for energies less than 3 MeV they inferred that there was no anomalous enhancement in fission cross section as the measured events for energies lower than this were all attributed to  $^{252}\text{Cf}$  contamination of the chamber. Later there were measurements [11] of the fission cross sections in

alpha-particle induced fission of  $^{232}\text{Th}$ , utilizing a similar kinematic coincidence technique with a pair of position sensitive avalanche counters, which showed appreciable enhancements in fission cross sections in the ESBE region compared to that expected on the basis of a coupled channel calculations (CCFUS). It is, therefore, of interest to study the fission cross sections in the extreme sub-barrier energy region. In the present work, we have carried out systematic measurements of the fission cross sections at the extreme sub-barrier energy region for different systems to investigate fusion-fission, transfer induced fission, and low momentum transfer fission events to understand further the fission process at large internuclear distances. The fission cross sections in  $^{11}\text{B}$ ,  $^{16}\text{O}$ ,  $^{19}\text{F}+^{232}\text{Th}$  reactions have been measured employing the kinematic coincidence technique with two large area X-Y position sensitive multiwire avalanche counters to separate the fission events corresponding to FF, TF, and LMTF events over a large range of bombarding energies extending to ESBE region. This technique has the advantage that the linear momentum of the fissioning nucleus can be determined from the folding angle of the two fragments thereby obtaining information about the reaction processes that contribute to fission in different energy regions.

Most of the previous measurements of fission cross sections in heavy ion induced reactions in the ESBE region have been inclusive measurements, which did not distinguish compound nuclear fission (fusion-fission FF) and noncompound nuclear fission events. It is known [12] that at sub-barrier energies, fission following transfer of one or more nucleons from projectile to the target (transfer fission TF) competes with FF and that their contributions can be separately determined by measuring the linear momentum transfer to the fissioning nucleus with the help of the folding angle technique. It was shown in Ref. [12] that at sub-barrier energies due to the backward peaking of the ejectile angular distributions, the transfer induced fission events correspond to larger linear momentum as compared to FF, giving rise to the TF peak at smaller folding angles than the FF peak. The low momentum transfer events will correspond to folding angle of nearly  $180^\circ$  and can be separated easily from the above two modes of fission. In the present measurements also, we find an appreciable number of fission events corresponding to low momentum transfer. Several control experiments were carried out to estimate the contribution due to secondary neutron background to the observed LMTF events. The results on the cross sections of different types of fission (FF, TF, and LMTF) processes are presented and discussed below.

The experiments were performed with  $^{11}\text{B}$  (19–65 MeV),  $^{16}\text{O}$  (55–80 MeV),  $^{19}\text{F}$  (55–80 MeV) beams from the BARC-TIFR 14UD Pelletron accelerator at Mumbai. A self-supporting  $1.8\text{ mg/cm}^2$  thick  $^{232}\text{Th}$  target was used in the experiment to measure the fission fragments in back-to-back geometry. Two low pressure X-Y position sensitive multiwire avalanche counters of Breskin-type, having active dimensions of  $6.5\text{ cm}$  by  $5.0\text{ cm}$  and  $15\text{ cm}$  by  $3.5\text{ cm}$ , were mounted on either side of the fissile target for detecting the complementary fission fragments in coincidence. The PSD's were kept at  $14\text{ cm}$  and  $12\text{ cm}$ , respectively, from the target subtending the in-plane angles of about  $26^\circ$  and  $63^\circ$ , respectively, at the target. The detectors were moved to different

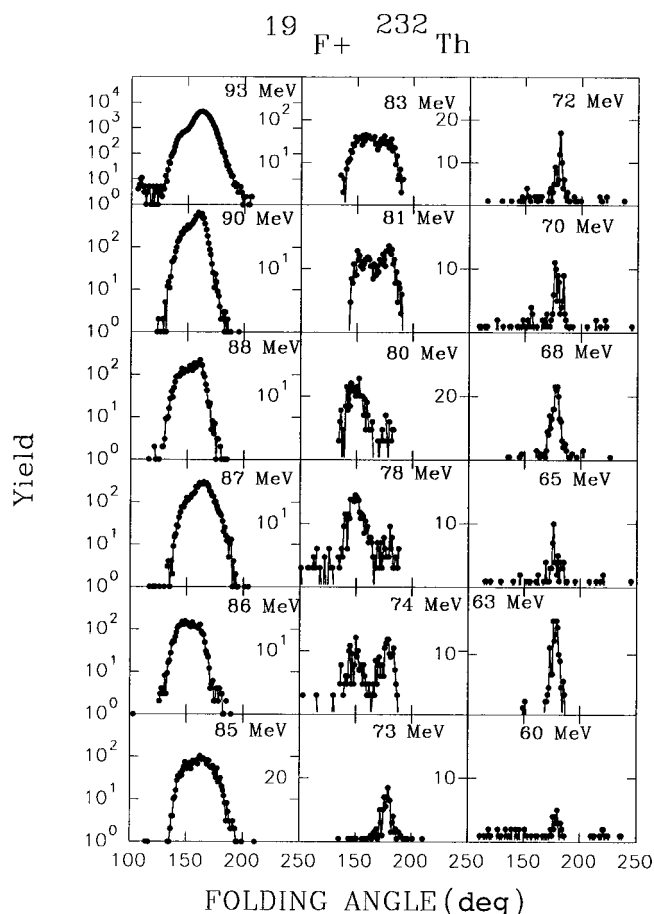


FIG. 1. Folding angle distribution for  $^{19}\text{F}+^{232}\text{Th}$  system at various bombarding energies.

specified angles ( $33^\circ, 200^\circ$ ), ( $75^\circ, 253^\circ$ ) with respect to beam direction to carry out the measurements over a large angular range. The detectors were operated with isobutane gas at 2 torr pressure and provided excellent timing, position sensitivity, and pulse height discrimination of fission fragments from the beam-like particles. The time of arrival of the fragments at the two PSD's and the X and Y position pulses from the two detectors were recorded event by event in list mode. A 500 micron-thick semiconductor detector was placed at  $25^\circ$  at a distance of 40 cm from the target to monitor the elastically scattered heavy ions for normalization purposes.

The angle calibration of the fission fragment detectors was achieved from the observed dips in the fragment yields in the detectors due to the shadowing caused by the wires used to support the thin windows of the PSD's. This calibration was done using a  $^{252}\text{Cf}$  source mounted at the point of the target location. The coincidence timing information from the two fission fragment detectors was recorded as one of the parameters to select the genuine fission events ( $\Delta t < 20\text{ ns}$ ) and thus helped to reject random coincidences. From the event-by-event information on the position of the two complementary fragments in the two detectors, their angles of emission were calculated. The typical folding angle distributions for the case of  $^{19}\text{F}+^{232}\text{Th}$  at several bombarding energies are shown in Fig. 1. At higher bombarding energies, the folding angle distributions consist of two peaks, the dominant one being a near-Gaussian peak centered at a fold-

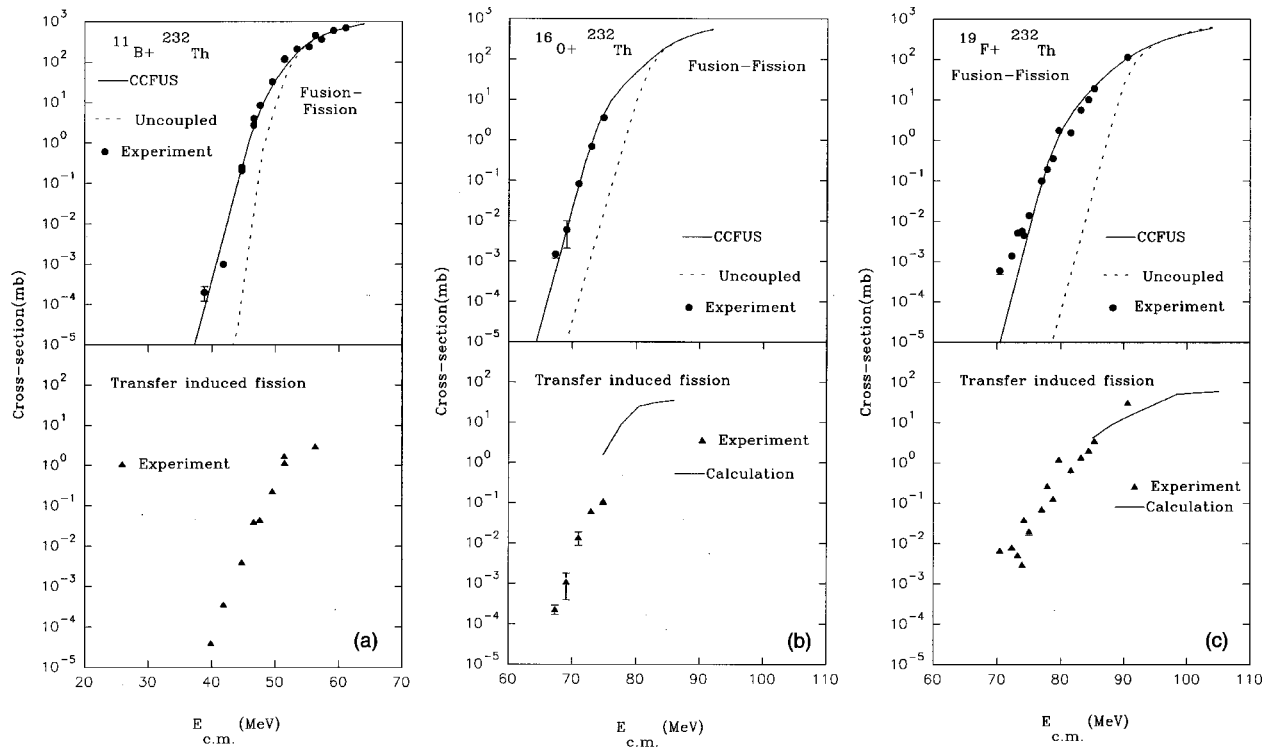


FIG. 2. (a)–(c) Measured fusion and transfer excitation functions for various systems. The continuous line and dashed lines represent the CCFUS calculations with and without calculations, respectively. In (b) and (c) the continuous line shown along with the transfer excitation function represent the calculations (see text).

ing angle corresponding to the expected position for the FF events. The folding angles for the fusion-fission events can be calculated on the assumption of full momentum transfer, symmetric mass division, and a total kinetic energy taken from Viola's systematics [13]. A second peak is observed at a lower folding angle which is attributed [11] to fission after transfer of a few nucleons, i.e., transfer fission (TF). As the energy is lowered in the sub-barrier energy region, the yield of TF relative to that of FF increases and, in addition, a distinct near-Gaussian third peak of comparable width (about  $8^\circ - 10^\circ$ ) peaked at large folding angle (about  $178^\circ - 180^\circ$ ) corresponding to low momentum transfer fission (LMTF) is observed in the ESBE region.

The measured folding angle distributions at different bombarding energies were fitted with three Gaussian peaks corresponding to the contributions from FF, TF, and LMTF events. The cross sections of FF and TF events thus determined at different bombarding energies are shown in Figs. 2(a)–2(c) for the three systems. The figures also show the results of the one-dimensional barrier penetration model and coupled channel model [14] calculations for the fusion cross sections in various systems. It is seen that the measured fusion-fission cross sections are enhanced by orders of magnitude in the sub-barrier region as compared to the one dimensional calculations. The coupled channel calculations are able to reasonably account for the sub-barrier cross sections except at the extreme sub-barrier energies for the  $^{19}\text{F} + ^{232}\text{Th}$  system, where the measured cross sections are still somewhat higher than the calculated values. The coupled channel calculations were done using CCFUS code [14] by including the axially symmetric deformation of the  $^{232}\text{Th}$  target ( $\beta_2 = 0.217$  and  $\beta_4 = 0.09$ ) and inelastic excitation channels of

the target and the projectile [5,15]. The disagreement of the experimental and calculated cross sections in the extreme sub-barrier regions ( $E/V_B \approx 0.7$ ) may suggest that the WKB transmissions used in the coupled channel models may not be valid [16], particularly if long range absorption contributions generated by the optical model potentials are appreciable. The fusion barrier distributions [5] derived from the fission cross sections using  $D(E) = d^2(E_{c.m.}\sigma)/dE_{c.m.}^2$  as a function of bombarding energy are shown in Fig. 3. The continuous lines show the results of CCFUS calculations. The results from earlier measurements [6] have been also included in the figure. It is seen that, in general, the calculated fusion barrier distributions are in agreement with the measured barrier distributions even at the lowest energies.

The results on TF cross sections have been plotted in the lower panels of Figs. 2(a)–2(c). The TF cross sections are also seen to decrease with decreasing energy but less steeply than that seen for the FF cross sections. Measurements [17] of energy and angular distributions of projectilelike particles for different projectiles on  $^{232}\text{Th}$  target also show that the ratio of total singles transfer cross sections ( $\sigma_{tr}$ ) to the total reaction cross section ( $\sigma_r$ ) also increases sharply at sub-barrier energies implying that at these energies there is a significantly large yield of transfer induced fission of the residual nucleus. The transfer fission cross sections were calculated from the measured transfer cross sections data and the fission probabilities given by the PACE2 code with level density parameters  $a_n = A/10 \text{ MeV}^{-1}$ ,  $a_f/a_n = 1.0$  and Sierk fission barriers, and are shown as continuous lines in Figs. 2(b) and 2(c) for the  $^{19}\text{F} + ^{232}\text{Th}$  and  $^{16}\text{O} + ^{232}\text{Th}$  reactions, where the transfer cross-section data are available to a lim-

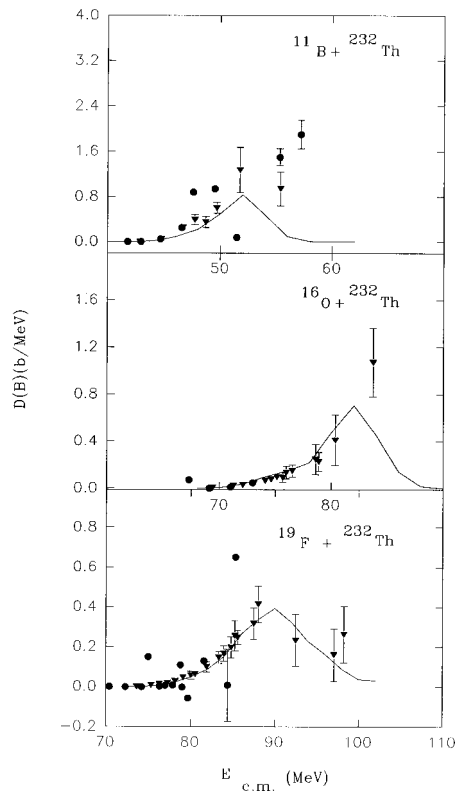


FIG. 3. Fusion barrier distributions for various systems. The inverted triangles are taken from Ref. [5]. The continuous line shows the CCFUS calculation.

ited extent. The trend in the TF cross section in  $^{19}\text{F}+^{232}\text{Th}$  and  $^{16}\text{O}+^{232}\text{Th}$  reactions is qualitatively reproduced by the calculations.

As mentioned earlier, in the ESBE region there are appreciable number of fission events observed for all the systems corresponding to very low momentum transfer (LMTF). The bombarding energy dependence of these events is seen to be rather weak as seen from the plot in Fig. 4, where the number of events normalized to the total integrated beam particles for each energy has been shown. The data have been collected over the energy range extending down to 30 percent below the barrier energy. The perseverance of the LMTF events even at the lowest energies is quite clearly seen, and one may expect the dominant contributions to come from the secondary fast neutron background induced fission in the  $^{232}\text{Th}$  target. With a view to check this aspect, we also measured simultaneously the fast neutron yields by means of a NE213 liquid scintillator detector (5 cm by 5 cm) kept at a distance of 25 cm from the target. The pulse shape discrimination property of the NE213 detector was utilized to separate neutron and gamma ray events. The threshold of neutron detector was kept at 100 keV electron equivalent energy using  $^{137}\text{Cs}$  and  $^{60}\text{Co}$  sources.

In order to estimate the contributions of neutron background to the observed fission events, experiments were carried out to measure simultaneously the neutron yields and fission yields under several control conditions such as (i) stopping the heavy ion beam just ahead of the fissile target by a thick stopper material upstream, (ii) allowing the beam to hit an Al stopper placed at the position of the fissile target, and (iii) allowing the beam to hit the beam dump placed

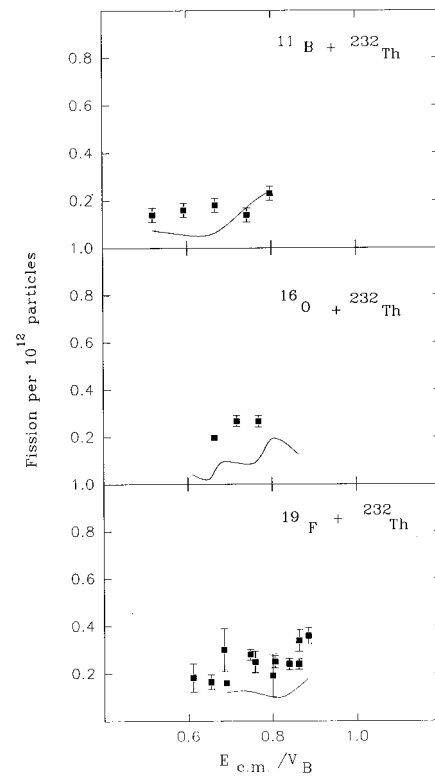


FIG. 4. The observed yield of LMTF events normalized for  $10^{12}$  particles for various systems. The continuous line indicates the yield expected based on measured neutron background.

about 1 m from the target. Neutron background induced fission events were also observed when the beam was allowed to hit the target ladder, which is made of steel. A quantitative estimate was made of the fissions induced by the background neutrons as observed during the experiment with appropriate correction factors for neutron detection efficiency, solid angle for neutrons at target location and the average  $^{232}\text{Th}(n,f)$  cross sections. Our estimates of this fast neutron induced background induced fission contribution assuming an average cross section,  $\sigma(n,f)$  of 100 mb are shown in Fig. 4 by the continuous lines. It is seen that although the observed LMTF events are to some extent explained by the background neutron induced fission at higher energies, there may still be a small excess in the energy range of  $E_{c.m.}/V_B \approx 0.6-0.8$ . In order to still confirm the estimation procedure for the neutron background induced fission, a separate experiment was also carried out in which a secondary  $^{232}\text{Th}$  target was placed at about 2 cm from the original target away from the primary heavy ion beam, but exposed to the neutron background produced near the target, and fission events originating from the second target were measured with a semiconductor detector. The events seen by this detector serve as a background monitor for the background neutron induced fission in the  $^{232}\text{Th}$  target. It was seen that the measured events from the secondary target are within the range of calculated values. In order to assess the presence of fissile impurities (such as  $^{235,233}\text{U}$ ) in the  $^{232}\text{Th}$  target another experiment was carried out with the thermal neutron beam from Dhruva reactor at BARC, Mumbai. No contamination of the fissile impurities was seen up to the detection limit of a few ppm, thereby eliminating the possibility of thermal

neutron fission contribution to the observed LMFT events.

Considering the uncertainties in the control experiments carried out to estimate fast neutron induced fission background and the fact that the absolute number of excess fission events are rather small and show only a weak dependence on energy, it is rather difficult to assign these events to a new process. It will be quite intriguing if the observed LMFT events cannot be fully accounted for by background neutron induced fission events. However, as mentioned earlier, there have been observations of large fission cross sections in other systems in the ESBE region [7–11]. The mechanism responsible for these LMFT events observed in the ESBE region is not known. However, among the possible processes which may be conjectured regarding their possible origin are (a) due to Coulomb excited target nucleus having lifetime long enough for the fissioning nucleus to get slowed down in the target before undergoing fission and (b) due to fission following low linear momentum neutron transfer from the projectile to the target nucleus with the latter undergoing fission. To estimate the neutron transfer fission (NTF) cross section there is a need to measure the neutron transfer cross sections in these systems in the ESBE region

and some work in this regard has been initiated by us. Recent calculations by Bonaccorso *et al.* [18] and a series of papers [19–22] show that one neutron transfer processes are observed up to extremely large distances of closest approach of the collision partners, e.g., 24 fm for  $^{238}\text{U}+^{238}\text{U}$  reaction and 27 fm in the  $^{238}\text{U}+^{197}\text{Au}$  reaction.

To sum up, we have measured the fission excitation functions in  $^{11}\text{B}$ ,  $^{16}\text{O}$ ,  $^{19}\text{F}+^{232}\text{Th}$  systems pertaining to fusion-fission and transfer-fission reactions over a large range of bombarding energy extending to extreme sub-barrier energies. The coupled channel calculations are able to account for the fusion-fission cross sections over a large energy range except in the extreme sub-barrier region for  $^{19}\text{F}+^{232}\text{Th}$  system, where the calculations somewhat underpredict the cross sections for several systems. The present studies also show an appreciable yield of low momentum transfer fission (LMFT) events at the extreme sub-barrier energies which seem to be mostly but not fully accounted for as being due to fission induced by background neutrons in the target. Further studies are required to investigate the mechanism responsible for these LMFT events observed in the ESBE region.

- 
- [1] M. Beckerman, *Phys. Rep.* **129**, 145 (1985).  
 [2] C. Y. Wong, *Phys. Rev. Lett.* **31**, 766 (1978).  
 [3] H. Esbensen, *Nucl. Phys.* **A352**, 147 (1981).  
 [4] C. H. Dasso *et al.*, *Nucl. Phys.* **A405**, 381 (1983); *Phys. Lett. B* **183**, 141 (1987).  
 [5] N. Majumdar *et al.*, *Phys. Rev. C* **51**, 3109 (1995); **53**, R544 (1996).  
 [6] N. Majumdar *et al.*, *Phys. Rev. Lett.* **77**, 5027 (1996).  
 [7] N. N. Ajitanand *et al.*, *Phys. Rev. Lett.* **58**, 1520 (1987); *Phys. Rev. C* **40**, R1854 (1989).  
 [8] N. N. Ajitanand, *Proceedings of the International Conference on Nuclear Reaction Mechanism*, Calcutta (World Scientific Singapore, 1989), p. 238.  
 [9] R. P. Anand *et al.*, *Proc. Nucl. Phys. Symp.* **33B**, 113 (1990).  
 [10] J. C. Gehring *et al.*, *Phys. Rev. C* **44**, R1 (1991).  
 [11] N. Majumdar and P. Bhattacharya, *Proc. DAE Nucl. Phys. Symp.* **36B**, 224 (1993).  
 [12] P. Bhattacharya *et al.*, *Nuovo Cimento A* **108**, 819 (1995).  
 [13] V. E. Viola, Jr., K. Kwiatowski, and M. Walker, *Phys. Rev. C* **31**, 1550 (1985).  
 [14] J. Fernandez-Neillo, C. H. Dasso, and S. Landowne, *Comput. Phys. Commun.* **54**, 409 (1989).  
 [15] E. N. Shrushikov, *Nucl. Data Sheets* **53**, 601 (1988).  
 [16] S. V. S. Sastry *et al.*, *Proceedings of the International Nuclear Physics Symposium (INPS-95)*, B-80 (1995).  
 [17] D. C. Biswas *et al.*, *Phys. Rev. C* **52**, R2827 (1995).  
 [18] A. Bonaccorso, Z. Zelazny, and E. Piasecki, *Z. Phys. A* **358**, 329 (1997).  
 [19] G. Wirth *et al.*, *Phys. Lett. B* **177**, 282 (1986).  
 [20] G. Wirthe *et al.*, *Z. Phys. A* **330**, 87 (1988).  
 [21] F. Funke *et al.*, *Z. Phys. A* **340**, 303 (1991).  
 [22] G. Wirth *et al.*, *Phys. Lett. B* **253**, 28 (1991).